Electronic transport studies of single-crystalline In_2O_3 nanowires

Daihua Zhang, Chao Li, Song Han, Xiaolei Liu, Tao Tang, Wu Jin, and Chongwu Zhou[a)]
Dept. of E.E.-Electrophysics, University of Southern California, Los Angeles, California 90089

(Received 4 October 2002; accepted 12 November 2002)

Single-crystalline In_2O_3 nanowires were synthesized and then utilized to construct field-effect transistors consisting of individual nanowires. These nanowire transistors exhibited nice n-type semiconductor characteristics with well-defined linear and saturation regimes, and on/off ratios as high as 10^4 were observed at room temperature. The temperature dependence of the conductance revealed thermal emission as the dominating transport mechanism. Oxygen molecules adsorbed on the nanowire surface were found to have profound effects, as manifested by a substantial improvement of the device performance in high vacuum. Our work paved the way for In_2O_3 nanowires to be used as nanoelectronic building blocks and nanosensors. © *2003 American Institute of Physics.* [DOI: 10.1063/1.1534938]

Because of its distinctive optical, chemical, and electronic properties, indium oxide is attracting more and more attention in applications ranging from optoelectronic devices to chemical sensors. Since the performance of such devices can be critically dependent on the dimension or the surface-to-volume ratio of the material, numerous studies have focused on the preparation and characterization of low-dimensional In_2O_3 structures in recent years. Parallel to the success with In_2O_3 thin film chemical sensing devices used to detect O_3,[1] CO,[2] H_2,[2,3] NH_3, NO_2,[3] and Cl_2[4] zero-dimensional In_2O_3 nanoparticles showing interesting photoluminescence properties have also been thoroughly studied.[5] However, although some quasi one-dimensional In_2O_3 structures have been successfully synthesized, such as In_2O_3 nanowires,[6,7] nanofibers,[8] nanobelts,[9] and nanotubes,[10] their electronic properties have been rarely reported. No electronic devices based on one-dimensional In_2O_3 structures have been fabricated and studied, despite their enormous potential to be used as nanoelectronic building blocks and sensors in ways similar to other semiconducting nanowires.[11,12]

Here we report our transport studies on field-effect transistors (FETs) made of individual In_2O_3 nanowires synthesized via a novel chemical vapor deposition method. Our devices exhibited pronounced gate dependence and well-defined linear and saturation regimes, which were only observed in conventional silicon metal–oxide–semiconductor FETs and carbon nanotube transistors.[13,14] Thermal emission was determined to be the dominating transport mechanism through the temperature-dependent measurements. Oxygen molecules adsorbed on the nanowire surface was found to have a profound effect on the transistor performance, as manifested by a tenfold increase in conduction, one order of magnitude increase in the transistor on/off ratio and a significant shift of the threshold voltage for the device measured in high vacuum compared to in air.

In_2O_3 nanowires were synthesized by a laser ablation process as described previously.[15] Figure 1 shows a scanning electron microscope (SEM) image of the In_2O_3 nanowires grown on a Si/SiO_2 substrate. As-grown In_2O_3 nanowires distributed uniformly across the substrate, and appeared homogeneous and straight with lengths up to several micrometers and diameters around 10 nm. The inset shows a transmission electron microscope (TEM) image of a single In_2O_3 nanowire with a diameter of 10 nm, where the In/Au alloy particle can be seen at the very tip of the wire. Our synthesis approach exploits two distinctive advantages of the VLS mechanism: single-crystalline products and precise diameter control by using monodispersed catalyst clusters. In contrast, many of the one-dimensional In_2O_3 structures reported previously were either polycrystalline or lacking precise diameter control around the range of 10 nm.[6,7,9,10]

To make In_2O_3 nanowire FETs, the nanowires on the Si/SiO_2 substrate were sonicated into a suspension in isopropyl alcohol and then deposited onto a degenerately doped silicon wafer covered with 500 nm SiO_2. Photolithography and successive Ti/Au deposition were used to pattern the source and drain electrodes to contact individual nanowires. The upper-left inset of Fig. 2 is an atomic force microscope (AFM) image showing an In_2O_3 nanowire between two Ti/Au electrodes. The channel length between the two electrodes is 2 μm. The Si substrate was used as a back gate. Figure 2 shows a typical FET $I-V_{ds}$ characteristic curve of the device at room temperature. Six $I-V_{ds}$ curves at V_g

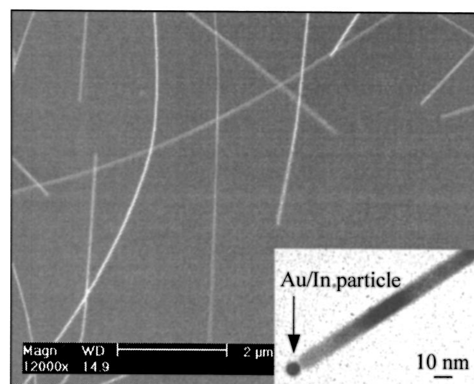

FIG. 1. A typical SEM image of In_2O_3 nanowires synthesized by laser ablation on a Si/SiO_2 substrate using monodispersed 10 nm Au clusters as the catalyst. The inset is a TEM image of an In_2O_3 nanowire with a catalyst particle at the tip. The scale bar is 10 nm.

[a)]Electronic mail: chongwuz@usc.edu

 © 2003 American Institute of Physics
Downloaded 06 Jan 2003 to 128.125.4.17. Redistribution subject to AIP license or copyright, see http://ojps.aip.org/aplo/aplcr.jsp

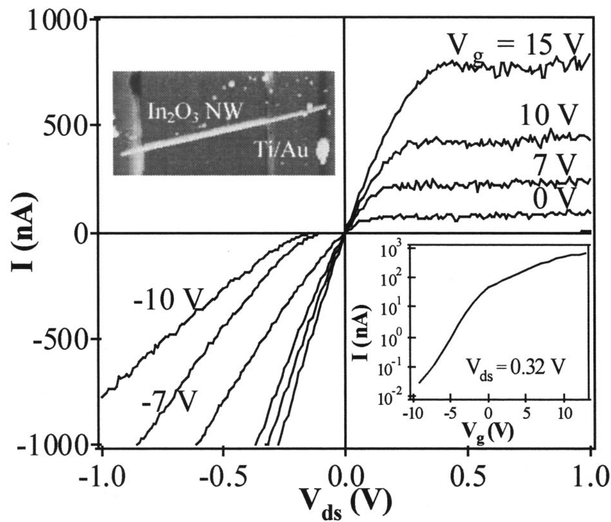

FIG. 2. Gate-dependent $I-V$ curves recorded at room temperature. The lower inset shows the current vs gate voltage at $V_{ds}=0.32$ V. The gate modulated the current by five orders of magnitude. The upper left inset is an AFM image of the In_2O_3 nanowire between two electrodes.

$=15$, 10, 7, 0, -7, and -10 V are displayed in this figure. With the gate voltage varying from $+15$ to -10 V, the conductance of the nanowire was gradually suppressed. From the slopes of the $I-V_{ds}$ curves at $V_{ds}=0$ V, we can see that the derivative conductance of the In_2O_3 nanowire at this bias was reduced from 3.13×10^{-6} S at $V_g=15$ V to 3.62×10^{-10} S at $V_g=-10$ V. In the positive drain-source bias region, the device was almost fully depleted at $V_g=-7$ V and $V_g=-10$ V. This behavior is in agreement with the well-known fact that In_2O_3 is an n-type semiconductor due to the O_2 deficiency. More interestingly, all the $I-V_{ds}$ curves exhibited asymmetric features with respect to the bias voltage. A case in point is the curve recorded at $V_g=0$ V. The current changed linearly with V_{ds} in the negative bias region, and reaches saturation when V_{ds} is greater than 0.1 V. A similar phenomenon was observed in p-type carbon nanotube transistor devices.[13,14] This saturation behavior is similar to the pinch-off effect in conventional silicon FETs: For an n-type semiconductor, a positive drain bias leads to a local depletion of carriers (i.e., pinch-off of the channel) around the drain because of the enhanced electric field across the gate oxide, and therefore saturation of the drain current is observed. On the other hand, a negative drain bias leads to a local enrichment of carriers around the drain, and hence, more conduction can be observed under negative V_{ds} than positive V_{ds} at the same gate bias. More information about this n-type transistor can be obtained from the $I-V_g$ curve shown in the lower-right inset. The curve was taken at $V_{ds}=0.32$ V, the current dropped dramatically from 6.54×10^2 nA at $V_g=14$ V to 3.15×10^{-2} nA at $V_g=-9$ V, indicating an on/off ratio of 2.08×10^4. We take $V_t=-9$ V as the threshold voltage necessary to completely deplete the nanowire. The carrier concentration along the wire is estimated to be 2.30×10^7 cm^{-1} following Ref. 16. The mobility of the carriers can be obtained to be 98.1 cm^2/V s. This mobility value compares well with a mobility of 3.17 cm^2/V s reported for B-doped Si nanowires,[12] indicating the high quality of our nanowires.

To further explore the electronic properties of the In_2O_3 nanowire device, we have measured the $I-V$ curves as a function of temperature, as shown in Fig. 3(a). These $I-V$ curves were taken at 290, 180, 120, 70, 30, and 10 K, respectively, with 0 V applied to the gate electrode. The conductance of this device decreased monotonically by several orders of magnitude as the temperature decreased. The current saturation at high source-drain bias was present throughout the temperature range we used; however, a new feature appearing as a gap around zero bias can be clearly seen for $I-V$ curves taken under 30 K. This suppression of conduction under small V_{ds} can be better viewed in Fig. 3(b), where the V_{ds} was swept within a small range (-0.10–0.10 V). We found that the conductance at $V_{ds}=0$ V was monotonically reduced with the decrease of temperature, from $G=7.08\times10^{-7}$ S at 290 K to $G=3.7\times10^{-10}$ S at 10 K. Figure 3(b) inset shows the zero-bias conductance versus $1/T$, where the dots are experimental data and the solid line is a fit calculated according to the formula $G\sim\exp(-E_a/k_BT)$, with a thermal activation barrier $E_a\sim6.90$ meV. This indicates that the transport through our device was dominated by thermal

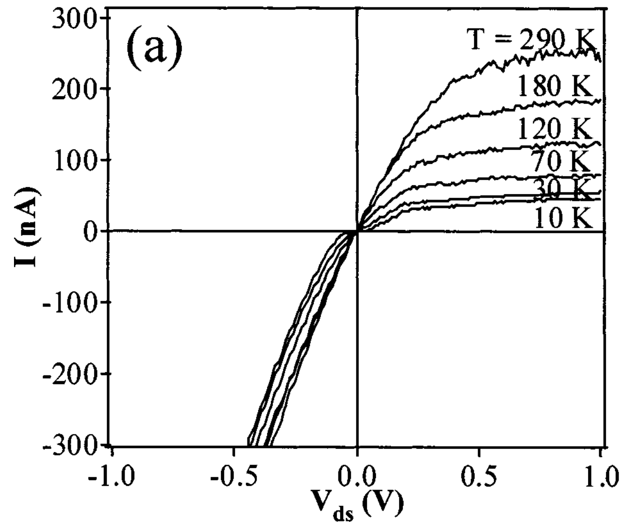

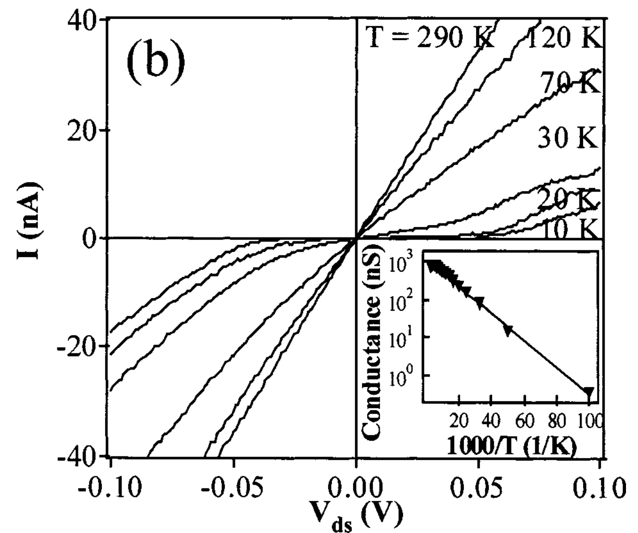

FIG. 3. (a) $I-V$ curves obtained at different temperatures at $V_g=0$ V. The corresponding temperatures were 290, 180, 120, 70, 30, and 10 K. (b) $I-V$ curve recorded in a small bias range ($V_{ds}=-0.1$ V$\sim+0.1$ V). Suppression of conduction around zero bias was observed in the curves for $T=20$ K and $T=10$ K. Inset: Conductance (in log scale) vs inverse temperature ($1/T$).

Downloaded 06 Jan 2003 to 128.125.4.17. Redistribution subject to AIP license or copyright, see http://ojps.aip.org/aplo/aplcr.jsp

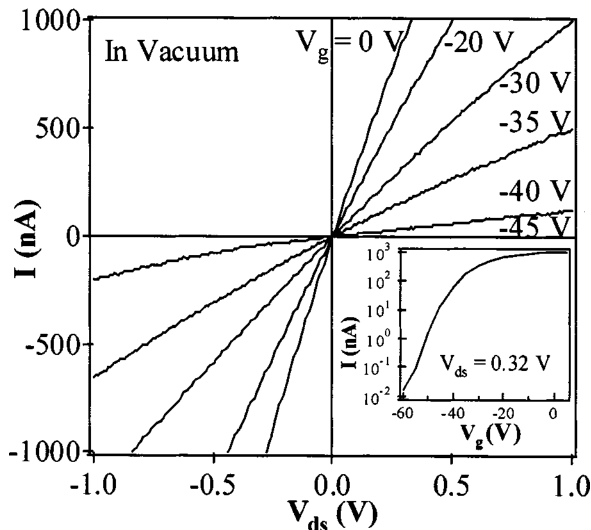

FIG. 4. Room temperature $I-V$ curves measured in a vacuum environment of 6×10^{-6} Torr. The inset shows the $I-V_g$ curve.

activation of electrons across the metal–semiconductor Schottky barrier. The barrier height of 6.90 meV was sufficiently low to produce ohmic behavior at room temperature; however, below the temperature of 20 K, where $k_BT<E_a$, thermally activated transport through the system was quenched and therefore a gap appeared in the small bias region around $V_{ds}=0$ V. At $T=10$ K, for an example, a gap between $V_{ds}=-40$ and 50 mV was observed and the sample was virtually insulating within this region under a zero gate bias. Larger $|V|$ brought the device into a conductive state again. The electron transport here is suggested to be dominated by the quantum-tunneling effect. Similar mechanisms were reported before.[13]

The sample was also loaded into a high vacuum chamber to study the effects of adsorbed molecules since this can be important for using In_2O_3 nanowires as chemical sensors. The gate-dependent $I-V$ curves taken in a vacuum of 6×10^{-6} Torr are shown in Fig. 4. Surprisingly, all the curves became linear, and the conductance was dramatically enhanced in the high vacuum environment. For instance, the current at $V_{ds}=0.5$ V, $V_g=0$ V measured in air was about 100 nA, as shown in Fig. 2; however, the current measured in vacuum exceeded 1 μA at the same V_{ds} and V_g, as shown in Fig. 4. To get the carriers fully depleted, we had to use a V_g as high as -55 V, compared to the threshold voltage of -9 V obtained in air. An on/off ratio $\sim10^5$ can also be derived from the same curve, compared to 2.08×10^4 obtained in air. Using the data obtained from the $I-V_g$ curve shown in the inset and the same calculation method described previously, the conduction electron density and the mobility were estimated to be $n=1.41\times10^8$ cm^{-1}, $\mu=46.9$ cm^2/V s, respectively. We believe that this "vacuum effect" is related to the O_2 in air. As mentioned in many semiconductor-oxide gas sensor references,[17,18] the oxygen molecules can adsorb on the In_2O_3 surface and undergo the following reaction with the conduction electrons: $O_2+e^-\rightarrow O^{2-}$.[19] This process takes electrons away from the material, generate a depletion layer at its surface and therefore suppresses the conductivity of the nanowires. By loading the device into a high-vacuum environment, O_2 molecules were pumped away from the In_2O_3 surface and, hence, higher carrier concentration and conduction were observed. Finally, we emphasize that we have measured several In_2O_3 nanowire transistors made using our synthesis and fabrication approach, and the data presented here including the gate dependence, the temperature dependence and the oxygen response are typical for all those devices.

In conclusion, we have made In_2O_3 nanowire transistors and studied their electronic properties. Our nanowires were confirmed to be n-type doped and exhibited nice transistor characteristics with well-defined linear and saturation regimes. On/off ratios as high as 2.08×10^4 and an electron mobility of 98.1 cm^2/V s were observed in air at room temperature. Temperature-dependent measurements revealed thermal emission as the dominant transport mechanism with an activation barrier of 6.90 meV. We have also found that high vacuum can dramatically improve the conduction of our In_2O_3 nanowires due to the desorption of oxygen molecules. Our results indicate that In_2O_3 nanowires have great potential to be used as nanoelectronic building blocks and ultrasensitive chemical sensors.

The authors thank Dr. Jie Han, Dr. Meyya Meyyapan, Professor Edward Goo, Professor Martin Gundersen, and Dr. Xiaodong Zhang for their help. This work is supported by USC, a Powell award, NASA Contract No. NAS2-99092, NSF CAREER award, NSF NER program, and a Zumberger award.

[1] E. Gagaoudakis, M. Bender, E. Douloufakis, N. Katsarakis, E. Natsakou, V. Cimalla, and G. Kiriakidis, Sens. Actuators B **80**, 155 (2001).
[2] W. Chung, G. Sakai, K. Shimanoe, N. Miura, D. Lee, and N. Yamazoe, Sens. Actuators B **46**, 139 (1998).
[3] M. Liess, Thin Solid Films **410**, 183 (2002).
[4] J. Tamaki, C. Naruo, Y. Yamamoto, and M. Matsuoka, Sens. Actuators B **83**, 190 (2002).
[5] H. Zhou, W. Cai, and L. Zhang, Appl. Phys. Lett. **75**, 495 (1999).
[6] M. Zheng, L. Zhang, G. Li, X. Zhang, and X. Wang, Appl. Phys. Lett. **79**, 839 (2001).
[7] X. Peng, G. Meng, J. Zhang, X. Wang, Y. Wang, C. Wang, and L. Zhang, J. Mater. Chem. **12**, 1602 (2002).
[8] C. Liang, G. Meng, Y. Lei, F. Phillipp, and L. Zhang, Adv. Mater. **13**, 1330 (2001).
[9] Z. Pan, Z. Dai, and Z. Wang, Science **291**, 1947 (2001).
[10] B. Cheng and E. T. Samulski, J. Mater. Chem. **11**, 2901 (2001).
[11] J. Kim, H. So, J. Park, J. Kim, J. Kim, C. Lee, and S. Lyu, Appl. Phys. Lett. **80**, 3548 (2002).
[12] Y. Cui, X. Duan, J. Hu, and C. M Lieber, J. Phys. Chem. B **104**, 5213 (2000).
[13] C. Zhou, J. Kong, and H. Dai, Appl. Phys. Lett. **76**, 1597 (2000).
[14] X. Liu, C. Lee, C. Zhou, and J. Han, Appl. Phys. Lett. **79**, 3329 (2001).
[15] C. Li, D. Zhang, S. Han, X. Liu, T. Tang, and C. Zhou, Adv. Mater. (to be published).
[16] R. Martel, T. Schmidt, H. R. Shea, T. Hertel, and P. Avouris, Appl. Phys. Lett. **73**, 2447 (1998).
[17] S. Strassler and A. Reis, Sens. Actuators **4**, 465 (1983).
[18] D. E. Williams, Sens. Actuators B **57**, 1 (1999).
[19] H. Kind, H. Yan, B. Messer, M. Law, and P. Yang, Adv. Mater. **14**, 158 (2002).

Downloaded 06 Jan 2003 to 128.125.4.17. Redistribution subject to AIP license or copyright, see http://ojps.aip.org/aplo/aplcr.jsp